

Fast Biofluid Transport of High Conductive Liquids Using AC Electrothermal Phenomenon, A Study on Substrate Characteristics

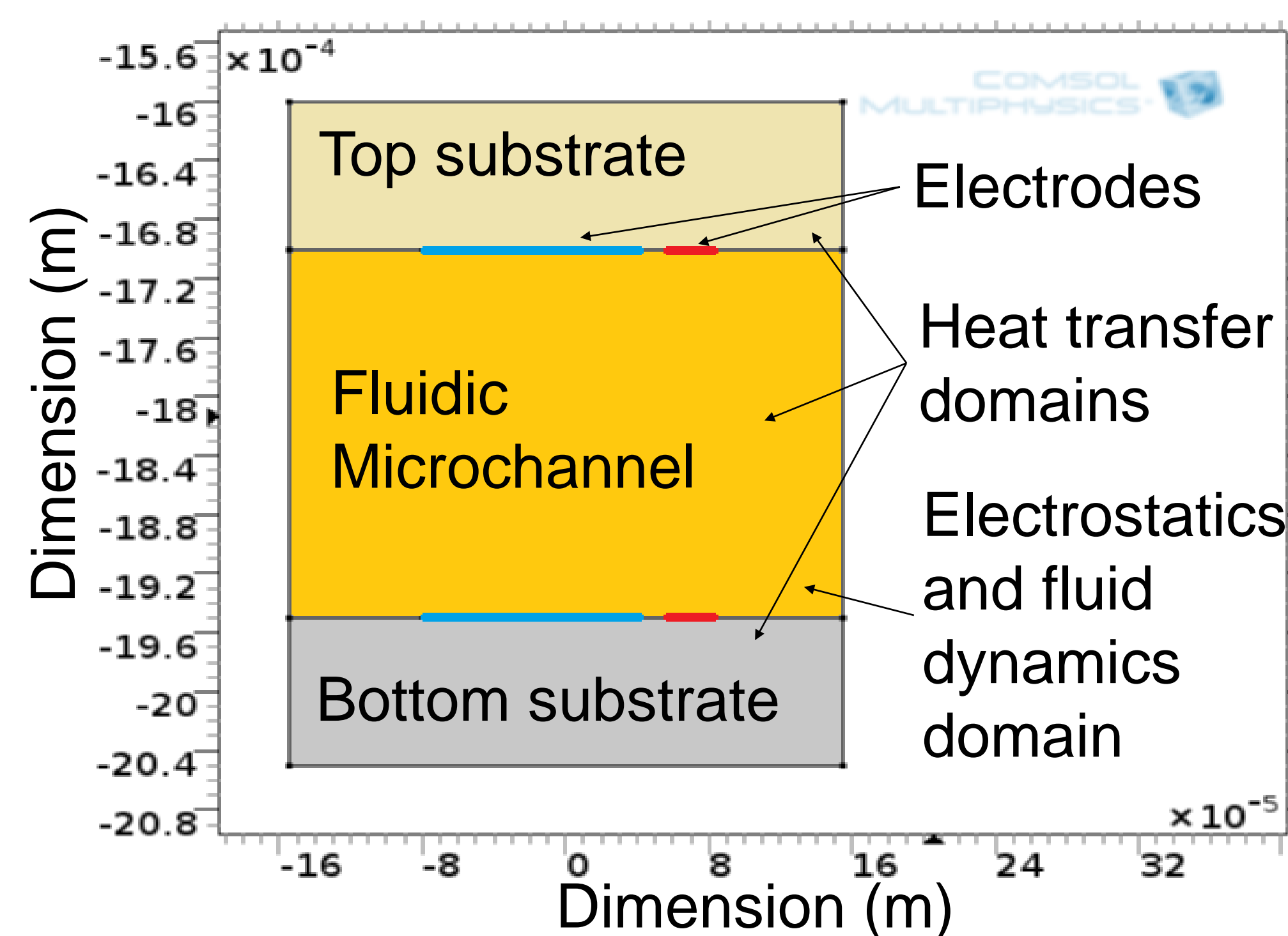
À Salari È Dalton

Ö] æq ^} of -Ö|^&c&æ/BÁÖ [] ~ c|ÁÖ} * ä ^^|ä * ÊÄV ä^|•ã Á -Öæ* æ^ , Calgary, AÖ, Canada

Introduction:

AC electrothermal flow is based on permittivity and conductivity gradients caused by Joule heating effect. Substrate thermal characteristics can affect the heat transfer throughout the system and consequently change the ACET micropump performance.

Figure. 1 The ACET micropump geometry



Computational Methods:

The ACET flow modeling includes:

- *Electrostatics* by solving Laplace equation to determine the electric field distribution;
- *Heat transfer* in liquids and solids by solving energy conservation equation to achieve the temperature gradient throughout the system;
- *Laminar flow* by solving Navier-Stokes equation to obtain the resultant ACET flow regime.

Results:

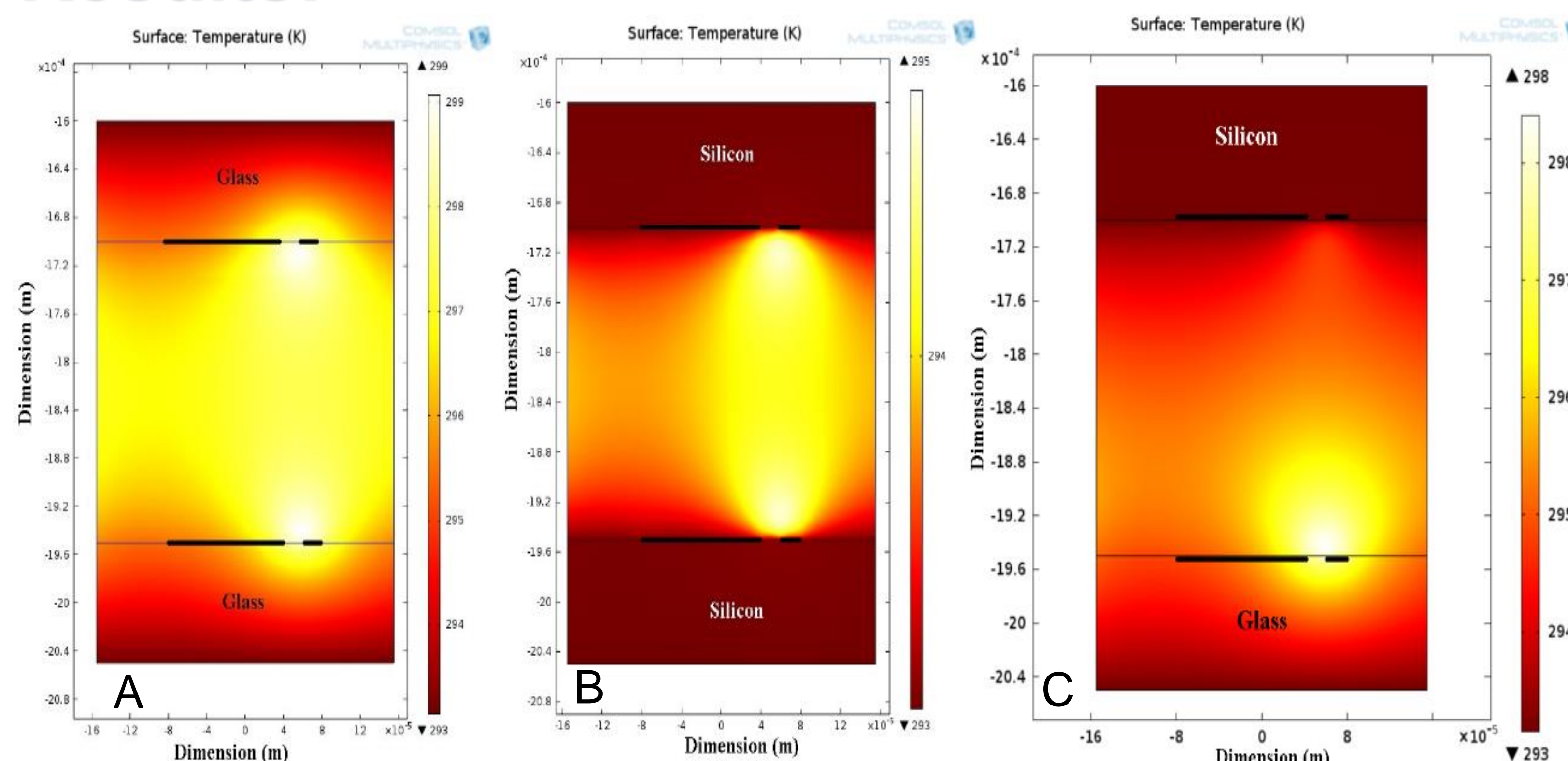


Figure. 2 Temperature distribution in three micropumps; (A): glass-glass; (B): silicon-silicon; (C): silicon-glass. Higher thermal conductivity of silicon causes it to sustain negligible temperature gradient, while $\approx 5^\circ\text{K}$ temperature drop is observed in glass substrate. $\text{freq}=100\text{ kHz}$, $\sigma=0.224\text{ S/m}$, $V_{rms} = 7$.

References:

1. R. Zhang, C. Dalton and G. A. Jullien, "Two-phase AC Electrothermal Fluidic Pumping in a Coplanar Asymmetric Electrode Array," *Microfluid. Nanofluid.*, 10, 521-529 (2011).
2. Q. Yuan, K. Yang and J. Wu, "Optimization of Planar Interdigitated Microelectrode Array for Biofluid Transport by AC Electrothermal Effect," *Microfluid. Nanofluid.*, 16, 167-178 (2014).
3. A. Salari, M. Navi and C. Dalton, "AC Electrothermal Micropump for Biofluidic Applications Using Numerous Microelectrode Pairs," in *IEEE CEIDP*, Des Moines, IA (2014).
4. E. Du and S. Manoochehri, "Microfluidic Pumping Optimization in Microgrooved Channels with AC Electrothermal Actuations," *Applied Physics Letters*, 96, 034102 1-3 (2010).
5. M. Lian, N. Islam and J. Wu, "AC Electrothermal Manipulation of Conductive Fluids and Particles for Lab-Chip Applications," *IET Nanobiotechnol.*, 1, 36-43 (2007).
6. M. Sigurdson, C. D. Meinhart and H. C. Feidman, "AC Electrothermal Enhancement of Heterogeneous Assays in Microfluidics," *Lab Chip*, 7, 1553-1559 (2007).

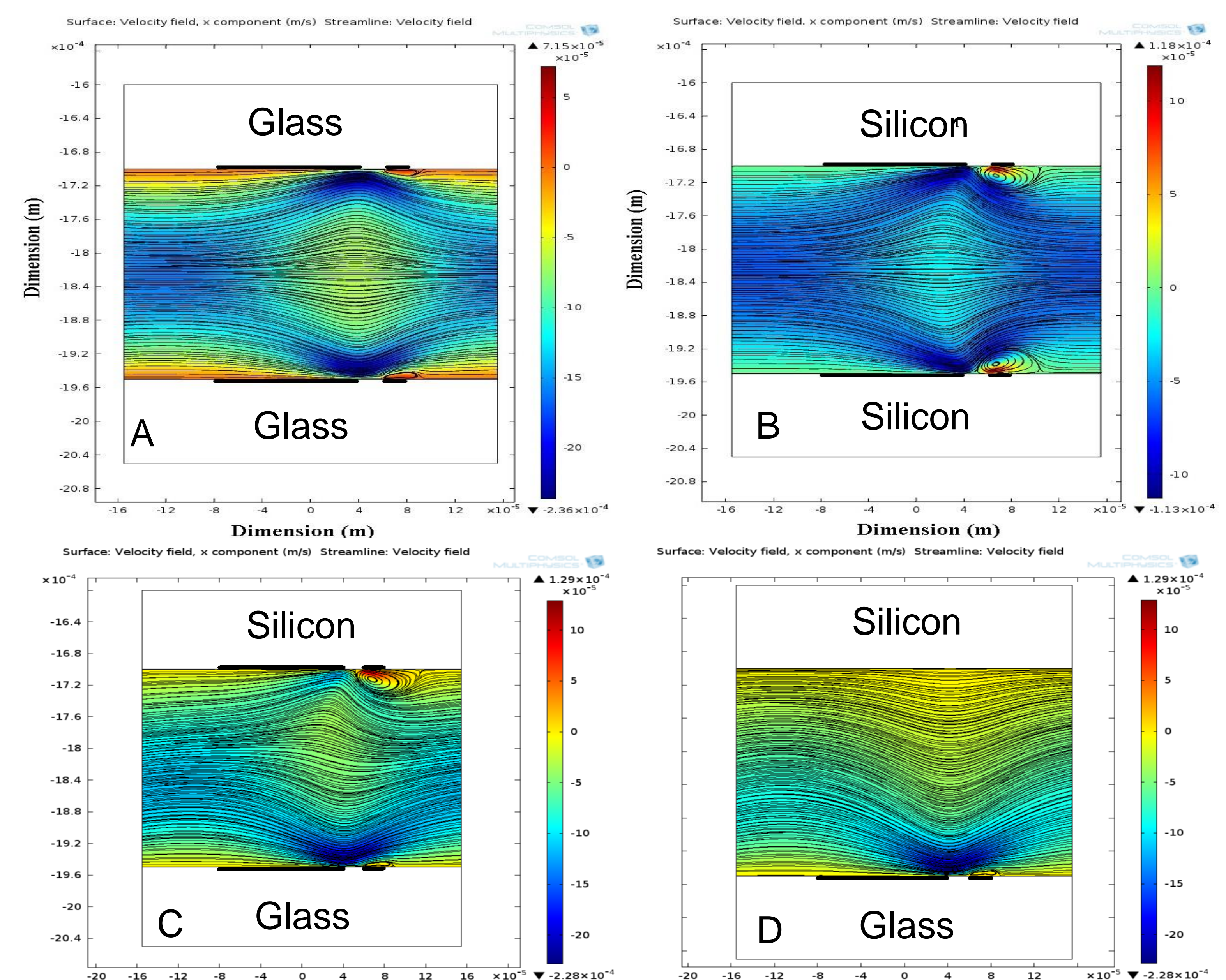


Figure. 3 ACET fluid flow for four different ACET micropump configurations; different substrate materials used as (A): glass-glass, (B): silicon-silicon, and (C): silicon-glass. (D): shows a micropump with one array of microelectrodes placed at the bottom of the fluidic microchannel. Glass-glass configuration provides the highest flow rates than the others. Also, maximum ACET velocity (x-component) occurs near the electrodes' edge. Moreover, net flow generated near the glass substrates suppresses the ACET vortices formed on top of the thin electrodes. This does not happen for the vortices near silicon substrates, as the net flow at this area has less strength. In all configurations, thin electrode is actuated at $V_{rms} = 7$, and wide one is grounded. $\text{freq}=100\text{ kHz}$, $\sigma=0.224\text{ S/m}$.

Conclusions:

- Maximum electric field and ACET flow velocity occur near the thin electrode;
- In ACET micropump with glass substrate the vortices generated near the electrode surfaces are suppressed causing in a higher net flow rate compared to that of silicon substrate;
- Increasing substrate thickness can increase the thermal resistance and cause higher flow rates up to 12%;
- Two-row electrode configuration increases the ACET velocity up to 200%.